THEORY OF HELIUM TRANSPORT AND CLUSTERING IN MATERIALS UNDER IRRADIATION *

N.M. GHONIEM [1], S. SHARAFAT [1], J.M. WILLIAMS [2] and L.K. MANSUR [3]

[1] School of Engineering and Applied Science, University of California at Los Angeles, Los Angeles, CA 90024, USA
[2] Solid State Division, Oak Ridge National Laboratory, Oak Ridge, TN 37830, USA
[3] Metals and Ceramics Division, Oak Ridge National Laboratory, Oak Ridge, TN 37830, USA

A theoretical model is developed to describe helium transport and clustering during irradiation. Diffusional reactions of helium with vacancies and vacancy clusters, with extended sinks for helium absorption, and direct reactions with displacement producing particles are included. The full description developed is employed in numerical computations. A simpler description is also developed in the limits where certain reactions are unimportant. Analytical expressions for the effective diffusion coeficient of helium are derived. Regimes of the parameter space of dose rate, temperature, helium generation rate, sink strength and other important conditions, where the effective diffusion coefficient is dictated by three different physical processes, are defined. The result is determined by the dominant release mechanism of helium bound in vacancies–thermal detrapping, replacement by the self-interstitial or direct displacement. Results from the full computations and the analytical expressions are compared.

1. Introduction

It has been demonstrated, through many experiments during the last decade, that the presence of helium atoms in metals and alloys is detrimental to their properties. It is also established that helium atoms assist the nucleation and growth of cavities in irradiated materials leading to volumetric swelling [1]. Helium migration and clustering at grain boundaries result in high temperature embrittlement [2]. Tensile and other mechanical properties are all shown to be influenced by the presence of helium [3].

Helium atoms introduced into the solid can reside in an interstitial position, in a substitutional position, or in clusters of helium and vacancies, which are at larger sizes termed cavities. Extensive computer simulation studies [4–6] have provided information on the energetics of helium reactions in the previously mentioned form.

Philipps and co-workers [7] concluded that the effective helium diffusion coefficient in nickel, D_{He}^{eff}, between 800 and 1250°C can be expressed as:

$$D_{He}^{eff} = 10^{-2.2 \pm 0.3} \exp\left(\frac{-0.81 \pm 0.04}{kT}\right), \qquad (1)$$

where k is Boltzmann's constant and T is temperature. The effective activation energy (0.81 eV) was interpreted as the difference between the dissociation energy of a helium atom in a substitutional site and the vacancy formation energy. More recently, evidence to the effect that the activation energy for diffusion of helium as an interstitial may be in the range of 0.11 to 0.14 eV [8, 9] has been obtained.

Under irradiation conditions, where helium atoms are introduced concurrently with displacement damage, three more features complicate the understanding of helium transport. First the competition between self-interstitials and helium atoms to react with vacancies. Next, helium atoms tend to agglomerate with radiation-induced as well as thermal vacancies. Finally, displacement collision cascades can supply enough energy to remove helium "bound" to vacancies or vacancy clusters. In this paper, we present a comprehensive model for the transport and clustering of helium in irradiated structural materials.

A comprehensive theory is presented in the next section including possible reactions influencing helium migration in irradiated structural materials. Since the interpretation on the numerical results involves various simplifications, an analytical model is given in section 3. While the numerical computations are essential, the analytical model describes the various regimes possible in terms of the parameters of the theory and give exact values of the effective diffusion coefficient in limiting

cases. Section 4 presents the results of the calculations. This is followed by discussions and conclusions in section 5. The symbols and notations are given in a separate "nomenclature" section.

2. Theory of helium transport

A major problem in formulating a theoretical model for helium migration lies in the complicated possibilities by which helium interacts with point defects. During irradiation, helium reactions include: (1) trapping and thermal detrapping of helium in single vacancies, divacancies and higher order clusters; (2) helium trapping at dislocations and grain boundaries; (3) replacement of helium bound to single vacancies by self-interstitials; (4) helium clustering into vacancy-helium complexes; (5) displacement of trapped helium atoms by irradiation; and (6) migration of helium as an interstitial atom or in a divacancy.

Ignoring the majority of the above possibilities, Reed [10] developed a simple model for helium diffusion in irradiated materials. In his model, helium was assumed to be thermally detrapped from irradiation produced vacancies. The effective helium diffusion coefficient was expressed as:

$$D_{He}^{eff} = \nu_{He} \frac{\lambda^2}{6} C_v^{-2/3} \exp\left(-E_{He}^D/kT\right). \tag{2}$$

In this study, we include all of the reactions outlined above. The basic assumption in our analysis is that helium-point defect interactions are homogeneous in time and space. As such, the discontinuous defect production nature due to the generation of collision cascades is not treated [11]. In the present model, reaction rate constants are derived by extending Chandrasekhar's earlier treatment of coagulation [12].

2.1 Rate equations

Chemical reaction rate theory is used here to describe clustering events between randomly migrating species. This method has been used previously to calculate nucleation rates of fission gas bubbles in nuclear fuels [13]. More recently, Russell and Hall [14] used chemical reaction rate theory to analyze point defect clustering in the presence of mobile helium. In order to calculate nucleation rates of helium–vacancy complexes, however, the mobility and binding energies must be included in the calculations. The detailed description of the time-dependent concentrations of helium–vacancy complexes is therefore essential. The influence

of helium migration on clustering and vica versa is the major difference between our approach and previous attempts [15–18].

The following set of equations describe the time-dependent concentrations of various helium–point defect clusters:

Unoccupied vacancies:

$$dC_{10}/dt = (1 - \varepsilon)G + Z_v^d D_v \rho_d (C_v^e - C_{10}) + gGC_{11}$$
$$+ (R_{I,20}C_{20} - R_{I,10}C_{10})C_I$$
$$+ \sum_{i=0}^{M} \sum_{j=0}^{N} (E_{ij}^v - R_{10,ij}C_{10})C_{ij}. \tag{3}$$

Self-interstitials:

$$dC_I/dt = G - \sum_{i=1}^{M} \sum_{j=0}^{N} R_{I,ij}C_{ij}C_I - Z_I^d \rho_d D_I C_I - 2R_{I,1}C_I^2. \tag{4}$$

Interstitial helium:

$$dC_{01}/dt = G_{He} - \left(Z_{He}^d D_{He}\rho_d + R_{10,01}C_{10}\right)C_{01}$$
$$+ Z_{He}^d D_{He}\rho_d C_{01}^e + R_{I,11}C_I C_{11}$$
$$+ \sum_{i=1}^{M} \sum_{j=1}^{N} \left(E_{ij}^{He} + jgG - R_{01,ij}C_{01}\right)C_{ij}. \tag{5}$$

Divacancies:

$$dC_{20}/dt = 0.5\left(\varepsilon G + R_{10,10}C_{10}^2\right)$$
$$- \left(\sum_{i=0}^{M} \sum_{j=0}^{N} R_{ij,20}C_{ij} + Z_{20}^d D_{20}\rho_d \right.$$
$$\left. + R_{I,20}C_I + E_{20}^v\right)C_{20}$$
$$+ \left(E_{30}^v + R_{I,30}C_I\right)C_{30} + E_{21}^{He}C_{21}. \tag{6}$$

Complexes containing m-vacancies and n-helium atoms:

$$dC_{mn}/dt = E_{m,n+1}^{He}C_{m,n+1} - \left(\sum_{i=0}^{M} \sum_{j=0}^{N} R_{ij,mn}C_{ij} \right.$$
$$+ Z_{mn}^d D_{mn}\rho_d + ngG + R_{I,mn}C_I$$
$$\left. + E_{mn}^{He} + E_{mn}^v\right)C_{mn}$$
$$+ \left(E_{m+1,n}^v + R_{I,m+1,n}C_I\right)C_{m+1,n}$$
$$+ \sum_{\substack{i+k=m \\ j+l=n}} R_{ij,kl}C_{ij}C_{kl}. \tag{7}$$

Eqs. (3)–(7) are not amenable to analytical solutions in the present form. Gear [19] implicit multistep numerical integration methods are therefore used for the solution of this set of stiff equations. A brief outline of the calculational method for the reaction rates of the previous set of equations is given below. It is important to note that in eqs. (3)–(7) reactions in the double sum over i and j should be implemented only once. Rates similar to $R_{00,mn}C_{mn}C_{00}$ are meaningless, and therefore are naturally not included. Also, reactions involving diffusivities of immoble species are set to zero.

2.2. Reaction rates

2.2.1. Impingement rates

In the jump method for calculating impingement rates, which is more suitable for small clusters [20], the reaction rate constant for the impingement is given by:

$$R_{\alpha,mn} = K_{mn}^{\alpha}\Gamma_{\alpha} \tag{8}$$

where K_{mn}^{α} = effective surface area/area per atom,

= combinatorial number for the interaction of mobile defect α with an m–n complex,

Γ_{α} = jump frequency of defect α,

$$= \nu_{\alpha}\exp(-E_{\alpha}^{M}/kT). \tag{9}$$

The effective surface area is written in terms of an effective trapping radius (R_{tr}) and the area per atom:

$$K_{mn}^{\alpha} = 4\pi R_{tr}^{2}/\lambda^{2}. \tag{10}$$

The combinatorial number K_{mn}^{α} can be dependent on a number of variables, such as the sink concentration and temperature.

In order to determine the combinatorial numbers, we consider two groups of cavities. In the first group, $m > n$ (number of vacancies is larger than the number of helium atoms per cluster), and in the second group $m < n$. For the case $m > n$, the cavity is taken to be like a void, and the trapping radii of these clusters for mobile species can be determined from the bias calculations of Wolfer and Ashkin [21]. The effective trapping radius, R_{tr}, is related to the bias factor, Z, by:

$$R_{tr}^{eff} = R(m)Z(m), \tag{11}$$

where $R(m)$ is the physical radius of the cluster containing m vacancies. The bias factor $Z(m)$ is calculated directly from ref. 21. When $m < n$, cavities will contain more helium than vacancies and a different approach is used. Based upon thermal desorption measurements, Kornelson and Gorkum [22] proposed an empirical equation for the effective trapping radius of the cluster.

This is expressed as:

$$R_{tr}(n) = R_{0}\{[1 + 0.25(1 + n)]\} \qquad 1 < n < 10, \tag{13}$$

where R_{0} is the physical radius of the cluster.

2.2.2. Emission rates

Two different approaches have usually been used to determine the emission rates, E_{mn}^{v} and E_{mn}^{He}. The first method as proposed by Wiedersich et al. [15] is based on the detailed balance on a hypothetical equilibrium Boltzmann distribution of voids. This approach is sometimes referred to as the classical drop model. The emission rate is given by

$$E_{mn}^{v} = K_{mn}^{v}\nu_{v}\exp(-E_{v}^{M}/kT)C_{v}^{e}\exp(-\Delta F/kT), \tag{13}$$

where ΔF is the free energy change in the emission process. The free energy is calculated using the Wiedersich–Hall [16] model, where ΔF depends on the surface energy and the work done on the helium gas. When the cluster size is small, this approach may not be valid.

Small-size vacancy–helium clusters are treated by a different method in our analysis. The emission rate of a vacancy is given by:

E_{mn}^{v} = (number of sites for emission)

× (vibrational frequency)

× (probability of dissociation)

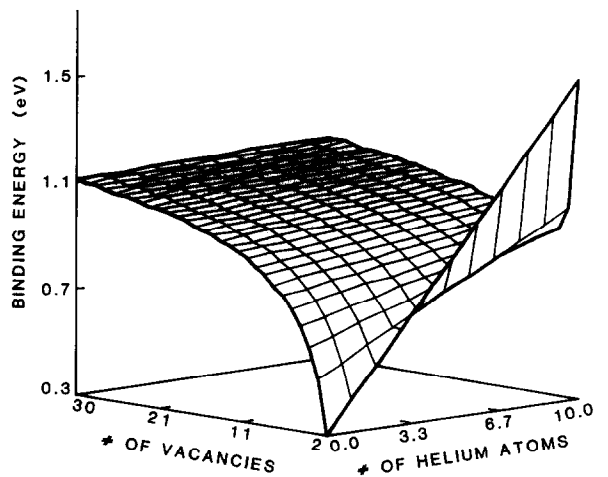$$= K_{mn}^{v}\nu_{v}\exp\left[-\left(E_{v}^{B} + E_{v}^{M}\right)/kT\right]. \tag{14}$$

Fig. 1. Binding energy of the last vacancy in a vacancy–helium complex as a function of the number of the vacancies and helium atoms in the complex.

Comparing eqs. (13) and (14), the energy needed for the binding of the last vacancy to a cluster containing m vacancies and n helium atoms is therefore given by:

$$E_B^v = \Delta F + E_F^v. \tag{15}$$

The binding energy E_B^v is shown in fig. 1 as a function of the number of of vacancies and helium atoms in a cluster. The thermal emission rates of helium atoms are calculated in a similar way [23]. Values calculated using eq. (15) are in basic agreement with refs. 5, 6, 25–27.

Finally, the coefficients for the migration of mobile species to sinks are calculated from their jump frequencies Γ, using the relationship:

$$D_\alpha = f_\alpha \lambda_\alpha^2 \Gamma_\alpha, \tag{16}$$

where f_α is a numerical factor of order unity and λ_α is the jump distance for defect α.

3. Analytical model for helium transport

While the set of eqs. (3)–(8) describes the basic features of helium and point defect interactions, it must be numerically integrated under any given condition. This can be computationally tedious, if the most important underlying physics is not clearly brought out. To guide the numerical computations by defining the several parameter regimes, and to find exact expressions for the helium effective diffusion coefficient in limiting cases, we present a simplified analytical model in this section This method is based on the one developed for the effective diffusion coefficient of point defects in the presence of impurities, as described by Mansur [28]. The basic assumptions of the present model are:

(1) The system is considered to contain the following defects: interstitial helium atoms, substitutional helium atoms, vacancies, self-interstitials, dislocations and a cavity size distribution.

(2) This system is in quasi-equilibrium (steady-state), and the results are applicable for times greater than a vacancy mean life-time.

(3) Nucleation and clustering are ignored, existing cavities are only in a state of growth.

(4) Divacancy population is negligible.

3.1. Simplified steady-state rate equations

Unoccupied vacancies:

$$G + G_T + E_{11}^{He}C_{11} + gGC_{11} - R_{1,10}C_{10}C_1$$
$$- R_{01,10}C_{01}C_{10} - K_{10}C_{10} = 0, \tag{17}$$

where

G_T = thermal vacancy generation rate,

$$= D_v C_v^e \left\{ Z_v^d \rho_d + 4\pi \int r_c N(r_c) Z_v^c \right.$$
$$\left. \times \exp\left[\left(\frac{2\gamma}{r_c} - P_g \right) \frac{\Omega}{kT} \right] \right\} dr_c, \tag{18}$$

$$K_{10} = D_v \left(Z_v^d \rho_d + 4\pi \int r_c N(r_c) Z_v^c dr_c \right). \tag{19}$$

Self interstitials

$$G - R_{1,10}C_{10}C_I - R_{1,11}C_{11}C_I - K_I C_I = 0, \tag{20}$$

where

$$K_I = D_I \left(Z_I^d \rho_d + 4\pi \int r_c N(r_c) Z_I^c dr_c \right). \tag{21}$$

Interstitial helium

$$G_{He} + E_{11}^{He}C_{11} + R_{1,11}C_I C_{11} - D_{He} Z_{He}^d \rho_d C_{01}$$
$$+ D_{He} Z_{He}^d \rho_d C_{01}^e$$
$$+ \int \left[E^{He}(r_c) + jgG - R_{01,r_c}C_{01} \right] 4\pi r_c N(r_c) dr_c$$
$$- R_{01,10}C_{01}C_{10} = 0. \tag{22}$$

Substitutional helium

$$R_{01,10}C_{01}C_{10} - E_{11}^{He}C_{11} - gGC_{11} - R_{1,11}C_{11}C_I = 0. \tag{23}$$

Eqs. (17), (20), (22) and (23), are special cases of eqs. (3), (4), (5) and (7), respectively.

Understanding helium clustering and transport under irradiation can be accomplished by the simultaneous solution of the set of eqs. (3)–(7). When clustering and divacancies are neglected, the solution of eqs. (17)–(23) provides a simplified insight into the problem of helium transport at steady-state. An effective helium diffusion coefficient for helium migration is defined as:

$$D_{He}^{eff} \sum_{m=0}^{M} \sum_{n=0}^{N} C_{mn} = \sum_{m=0}^{M} \sum_{n=0}^{N} D_{mn}C_{mn}, \tag{24}$$

where the sums in eq. (24) are only for mobile species. This definition for D_{He}^{eff} has been used to describe the results for both analytical and numerical calculations. In the special case where helium is transported only as either an interstitial or substitutional atom, eq. (24) simplifies to:

$$D_{He}^{eff} = \frac{D_{01}C_{01}}{C_{11} + C_{01}}, \qquad \text{for } D_{11} \ll D_{01}. \tag{25}$$

Solving eq. (23) for C_{01}, and substituting back in eq.

(25):

$$D_{He}^{eff} = \frac{D_{01}\left(E_{11}^{He} + gG + R_{1,11}C_I\right)}{\left(R_{01,10}C_{10} + E_{11}^{He} + gG + R_{1,11}C_I\right)}. \tag{26}$$

Eq. (26) gives the effective diffusion coefficient of helium in terms of the following quantities: the interstitial helium diffusion coefficient, the helium–vacancy binding energy, capture radii for point defect reactions, the helium radiation displacement rate; and the vacancy and interstitial concentrations and diffusion coefficients. In the following, we will analyze limiting cases for the solution of eq. (26).

3.2. Helium effective diffusion coefficient in limiting cases

3.2.1. Domination by thermal detrapping
In this case, the thermal dissociation rate of substitutional helium is greater than the interstitial replacement rate and the radiation displacement rate. Eq. (26) therefore becomes:

$$D_{He}^{eff} = \frac{D_{01}E_{11}^{He}}{R_{01,10}C_{10} + E_{11}^{He}} \tag{28}$$

substituting for E_{11}^{He} [eq. (15) applied to helium], $R_{01,10}$ [eq. (9)] and setting C_{10} = thermal equilibrium vacancy concentration; we obtain

$$D_{He}^{eff} = \frac{\alpha \exp\left[-\left(E_{He\,v}^B + E_{He}^M - E_v^f\right)/kT\right]}{1 + \beta \exp\left[-\left(E_{He\,v}^B - E_v^f\right)/kT\right]}, \tag{29}$$

where

$$\beta = K_{11}^v/K_{01}^{10} \exp\left(S_v^F/k\right) \tag{30}$$

and

$$\alpha = \beta D_{He}^0 \tag{31}$$

This equation reverts to the expression derived by Philipps and co-workers [7] for $E_{He\,v}^B > E_v^f$

3.2.2. Domination by replacement reaction
When the irradiation temperature is low enough or the dose rate is high enough for thermal detrapping to be negligible, substitutional helium is detrapped mainly by the effect of irradiation. This may be by direct irradiation displacement or indirect by self interstitials replacing He in substitutional sites. We will now derive an approximate expression for the latter case. Under these conditions, Eq. (26) becomes

$$D_{He}^{eff} = \frac{D_{01}R_{1,11}C_I}{R_{01,10}C_{10} + R_{1,11}C_I} \tag{32}$$

substituting for $R_{1,11}$, $R_{01,10}$, and D_{01}, we obtain

$$D_{He}^{eff} = \frac{\nu_{He}\lambda^2\,e^{-E_{He}^M/kT}K_{11}^I\nu_I\,e^{-E_I^M/kT}C_I}{k_{11}^I\nu_i\,e^{-E_I^M/kT}C_I - K_{10}^{01}\nu_{He}\,e^{-E_{He}^M/kT}C_{10}}. \tag{33}$$

However, at steady-state

$$\bar{Z}_I D_I C_I = \bar{Z}_v D_v\left(C_{10} - \overline{C}_v^e\right), \tag{34}$$

where $\overline{C}_v^e$ is the average thermal vacancy concentration and the Z's are weighted averages of the sink capture efficiencies. When several not too stringent conditions are satisfied, the helium effective diffusion coeficient takes a much simpler form. Under the following conditions:

$$C_{10} \gg \overline{C}_v^e, \qquad E_{He}^M \ll E_v^M, \qquad \bar{Z} = \bar{Z}_I \tag{35}$$

the effective helium diffusion coefficient simplifies to

$$D_{He}^{eff} = \eta D_v, \tag{36}$$

where $D_v \equiv D_{10}$ = vacancy diffusion coefficient, and η is a factor of order unity; $\eta = K_I^{11}/K_{01}^{10}$.

3.2.3. Domination by displacement reaction
When the rate of displacement of helium from vacancies is greater than both the thermal dissociation and the self-interstitial replacement rates eq. (26) becomes:

$$D_{He}^{eff} = \frac{D_{01}gG}{R_{01,10}C_{10} + gG}, \tag{37}$$

using eqs. (8) and (9) for $R_{01,10}$ the effective helium diffusion coefficient is

$$D_{He}^{eff} = \frac{D_{01}gG}{K_{10}^{01}\nu_{01}\exp\left(-E_{He}^M/kT\right)C_{10} + gG}. \tag{38}$$

In order to simplify eq. (38), an appropriate expression for C_{10} must be substituted. This depends on whether point defect concentrations are controlled by either mutual recombination or by diffusion to sinks. For mutual recombination to dominate, the following condition must be satisfied [24]

$$R = 4K_{01}^I G \exp\left(E_v^M/kT\right)/S_I S_v \nu_v \lambda^4 \gg 1. \tag{39}$$

If $R \gg 1$ (recombination dominated regime), the vacancy concentration, C_{10}, is given by [24]:

$$C_{10} \approx \left(\lambda^2 G\, S_I/K_{01}^I S_v\right)^{1/2} D_v^{-1/2} \tag{40}$$

substituting in eq. (38), and rearranging, we obtain

$$D_{He}^{eff} = \phi\left(GD_v\right)^{1/2}, \tag{41}$$

where

$$\phi = \frac{g}{\lambda K_{01}^{10}} \left(\frac{K_{01}^{I} S_v}{S_I} \right)^{1/2}. \tag{42}$$

In deriving eq. (41), the second term (gG) in the demoninator of eq. (38) is much than the first term, for any reasonable combination of parameters.

On the other hand, when point defect diffusion to sinks control point defect concentrations ($R \ll 1$), the vacancy concentration becomes

$$C_{10} \approx G/D_v S_v \tag{43}$$

and the effective diffusion coefficient in eq. (38) takes the form

$$D_{He}^{eff} = \psi D_v, \qquad \text{where } \psi = g\lambda^2 S_v/K_{01}. \tag{44}$$

3.3. Conditions for the validity of approximations

In this section, we will dereve formulas representing the conditions under which the previous approximate treatments of D_{He}^{eff} are valid.

3.3.1. Domination by thermal detrapping

In this case the thermal emission rate must be large.

$$K_{11}^{He} \nu_{He} \exp\left[-\left(E_{He}^{M} + E_{He\,v}^{B} \right)/kT \right] \gg gG,$$

$$\frac{K_{11}^{I}}{\lambda^2} D_I C_I. \tag{45}$$

This is satisfied when

$$nG \ll 1; \qquad n = \frac{g \exp\left[\left(E_{He}^{B} + E_{He}^{M} \right)/kT \right]}{K_{11}^{He} \nu_{He}}. \tag{46}$$

Also, the following conditions must be satisfied:

$$\varepsilon G \ll 1; \qquad \varepsilon = \frac{K_{11}^{I} \exp\left[\left(E_{He\,v}^{B} + E_{He}^{M} \right)/kT \right]}{K_{11}^{01} \lambda^2 \nu_{He} S_I} \tag{47}$$

for diffusion-limited point defect kinetics, and,

$$\xi G \ll 1;$$

$$\xi = \left(\frac{K_{11}^{I}}{K_{11}^{01}} \right) \frac{\nu_v \exp\left[2\left(E_{He}^{M} + E_{He\,v}^{B} - \frac{1}{2} E_v^{M} \right)/kT \right]}{\nu_{He}^2 K_{01}^{I}} \tag{48}$$

for recombination-limited point defect kinetics.

3.3.2. Domination by replacement reaction

$$R_{I,11} C_I \gg gG,$$

$$K_{11}^{He} \nu_{He} \exp - \left[\left(E_{He}^{M} + E_{He\,v}^{B} \right)/kT \right]. \tag{49}$$

This is satisfied when both

$$l \gg 1, \qquad \text{and } \varepsilon G \gg 1 \tag{50}$$

for sink-controlled point defect concentrations where

$$l = K_{11}^{I}/\lambda^2 g S_I. \tag{51}$$

For the case of recombination-limited point defect kinetics, the following must be satisfied:

$$mG^{-1/2} \gg 1, \qquad \text{and } \xi G \gg 1, \tag{52}$$

where

$$m = \frac{K_{11}^{I} \nu_v^{1/2}}{g} \exp\left(-\frac{E_v^{M}}{2kT} \right). \tag{53}$$

The results of eqs. (50) and (52) are straightforward substitutions in condition (49).

3.3.3. Domination by radiation displacement

$$gG \gg R_{I,11} C_I, \qquad K_{11}^{v} \nu_{He} \exp\left[-\left(E_{He}^{M} + E_{He\,v}^{B} \right)/kT \right] \tag{54}$$

Condition (54) is satisfied when both

$$l \ll 1, \qquad \text{and } nG \gg 1$$

for diffusion-limited point defect kinetics. For the case of recombination-limited kinectics, the following conditions must be satisfied:

$$nG^{-1/2} \ll 1, \qquad \text{and } nG \gg 1.$$

4. Results

It is computationally prohibitive to solve the previous set of numerical equations for the entire range of material and irradiation conditions possible. Moreover, dominant reaction mechanisms are not immediately clear. Therefore, we will first discuss the results of the analytical formulation, and then proceed to compare it to the more exact numerical computations.

Fig. 2 shows the dominant detrapping mechanisms at given combination of damage rate and irradiation temperature of well annealed nickel ($S_v \sim 10^9$ cm/cm^3). Recombination determines the kinetics of point defects for any combination of G and T above the line $R = 1$. The effective helium diffusion coefficient is determined therefore by thermal detrapping below the line $\xi G = 1$. Immediately above this line, self-interstitial replacement of trapped helium becomes the dominant mechanism. It is interesting to note that the higher the damage rate, the higher the dividing temperature between interstitial replacement and thermal displacement as detrapping mechanisms. This is effectively a temperature shift due to the higher displacement damage rate. Above this temperature the effective helium migration energy is the difference between the dissociation energy of bound
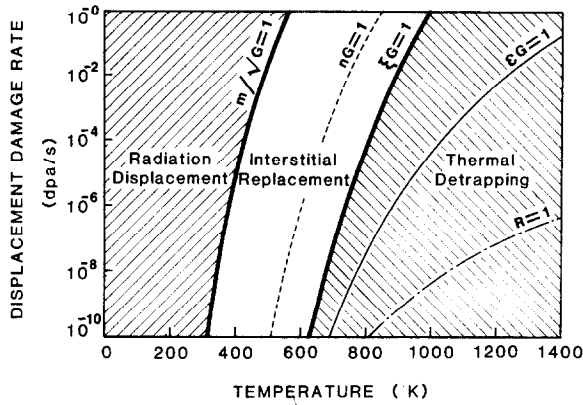
Fig. 2. Dominant detrapping mechanisms for given combinations of displacement damage rate and temperature at $S_v = 10^9$ cm/cm^3.

Fig. 4. The ratio of interstitial to vacancy flux for typical reactor conditions ($G = 10^{-6}$ dpa/s and $\rho_d = 10^{11}$ cm/cm^3), allowing for clustering and divacancy formation.

helium and the vacancy formation energy. Below this temperature the effective helium migration energy is roughly the vacancy migration energy. At still lower temperatures, radiation displacement takes over as a dominant detrapping mechanism. For example, the irradiation temperature has to be below 350 K for radiation displacement to be dominant under reactor conditions ($G = 10^{-6}$ dpa/s) and below 400 K under typical accelerator conditions ($G = 10^{-3}$ dpa/s). At higher effective sink densities, point defect concentrations are controlled by diffusion to sinks, except at very low temperatures. The dividing line for the temperature between self-interstitial replacement and thermal detrapping is therefore $\xi G = 1$ above the line $R = 1$, and $\varepsilon G = 1$ below the line $R = 1$, as shown in fig. 3.
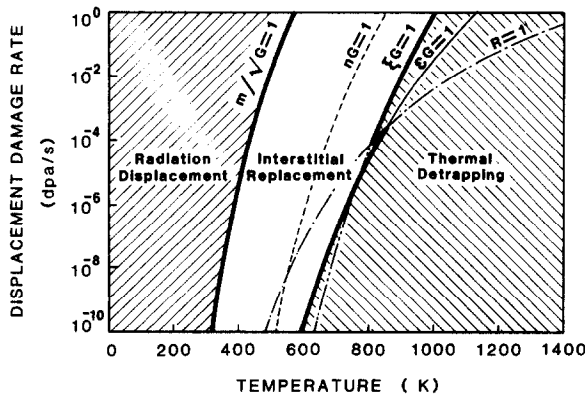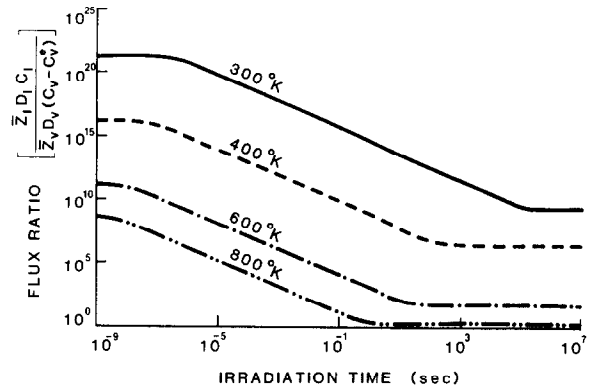
The validity of the analytical approximations is dependent on the attainment of conditions satisfying the basic assumptions. Many of the equations have been simplified by the assumption that the overall self-interstitial current to sinks is equal to the overall vacancy current to sinks. This is expressed as

$$\bar{Z}_I D_I C_I = \bar{Z}_v D_v (C_v - C_v^e);$$

the bias factors $Z_{I,v}$ being averaged over all sinks. This can be violated under two conditions. First, when the time interval is less than a few vacancy mean lifetimes; and second, when a fraction of the produced vacancies are retained in clusters that have a different mobility (divacancies), or immobile higher order clusters. Fig. 4 shows the ratio of the interstitial to vacancy flux, as
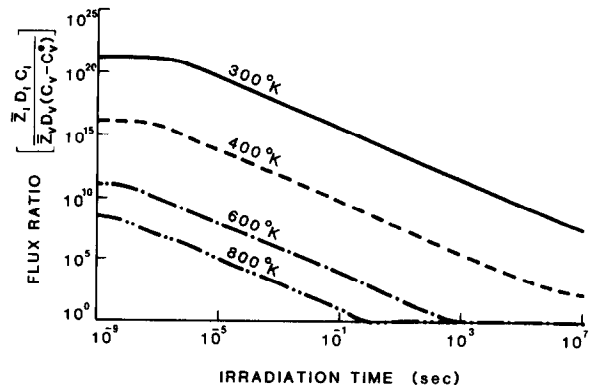

Fig. 3. Dominant detrapping mechanisms for given combination of displacement damage rate and temperature at $S_v = 10^{12}$ cm/cm^3.

Fig. 5. Ratio of interstitial to vacancy flux for typical reactor conditions ($G = 10^{-6}$ dpa/s and $\rho_d = 10^{11}$ cm/cm^3), without allowing for clustering and divacancy formation.
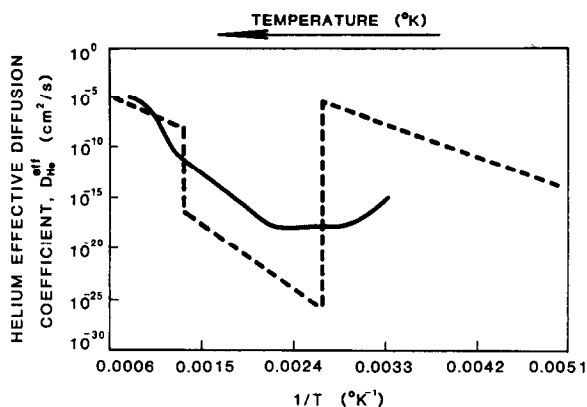
Fig. 6. Effective helium diffusion coeficient in nickel with no divacancies and no clustering. Dashed line is the analytical solution and solid line represents the numerical results.

Fig. 8. Effective helium migration energy as a function of irradiation temperature for nickel in typical reactor conditions when divacancies and vacancy–helium complexes are not allowed to form.

previously defined, for typical reactor irradiation conditions ($G = 10^{-6}$ dpa/s and $\rho_d = 10^{11}$ cm/cm^3) allowing for clustering and divacancy formation. It is shown that at higher temperatures (> 800 K), divacancy and multiple vacancy cluster formation is very weak and the flux ratio reaches approximately unity within seconds. However, at lower temperatures, the ratio is much larger than unity at the start of irradiation and then gradually decreases to a steady-state value that is still larger than unity. The basic reason for this is the formation of vacancy clusters that change the balance between vacancies and self-interstitials. In order to have numerical computations that are based on the same analytical model, the calculations were again performed without allowing for disvacancy or vacancy cluster formation, and the results are shown in fig. 5. It is clear that the assumptions of the analytical approach are valid for
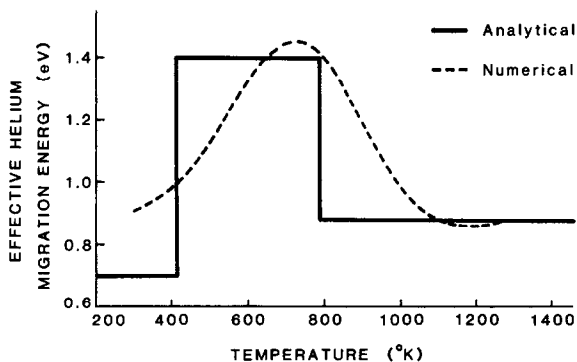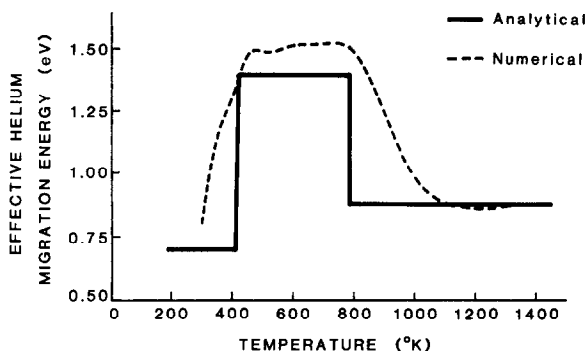

Fig. 7. Effective helium migration energy as a function of irradiation temperature for nickel at reactor conditions.

times greater than few vacancy mean lifetimes. However, this can be very long at low temperatures as shown in Fig. 5. The mobile self-interstitial flux is orders of magnitude greater than the vacancy flux at temperatures lower than 450 K and irratiation times less than roughly one year.

A comparison between the numerical calculations and the analytical approximation for the effective helium diffusion coefficient is shown in fig. 6. While the comparison is not meaningful at low temperatures because the point defect concentrations are still building up, it shows that the analytical solution can be used as a first order estimate of D_{He}^{eff}. The agreement is almost perfect at very high temperature where thermal detrapping is the only operating mechanism for helium release from traps. At intermediate temperatures, the combination of detrapping mechanisms makes the numerically evaluated D_{He}^{eff} higher than the analytical approximation.

Further comparisons between the two methods are shown in figs. 7 and 8. The effective helium migration energy during reactor irradiation for nickel is taken as the slope of D_{He}^{eff} versus T^{-1} as in fig. 6. Allowing for vacancy clustering and divacancy formation in the numerical model, the effective migration energy is given in fig. 7 as a function of temperature. Fig. 8 shows similar results when clustering and divacancies are suppressed in the numerical model. The agreement is reasonable in fig. 8, especially at the high temperature limit, and in that intermediate temperature regime. It is to be emphasized, however, that the analytical solutions are not intended to duplicate the more extensive numerical ones. Analytical estimates are used to explore mechanisms and to give a first order approximation to the exact value of D_{He}^{eff} under irradiation.

5. Conclusions

The problem of helium migration during the production of radiation damage is a critical one. Without understanding migration mechanisms and diffusion rates, it is hopeless to account for the fate of helium atoms injected or produced by structural alloys. This study provides two parallel and complementing approaches to the problem. An analytical formulation is developed, which is valid roughly above 350 K for reasonable reactor irradiation times (~ years). Below this temperature, the slow transient buildup in point defect concentration necessitates a time-dependent numerical solution. Under reactor irradiation conditions, the analytical model gives the following approximate values for helium effective migration energy in nickel:

$$(1) \quad E_{He}^{eff} \simeq 0.83 \text{ eV}; \left(E_{He}^{eff} \right.$$
$$\left. \simeq E_{He}^{B} + E_{He}^{M} - E_{v}^{F} \right) \ T \gtrsim 800 \text{ K},$$

$$(2) \quad E_{He}^{eff} = 1.4 \text{ eV}; \left(E_{He}^{eff} \simeq E_{v}^{M} \right)$$
$$400 \text{ K} \leq T \leq 800 \text{ K},$$

$$(3) \quad E_{He}^{eff} = 0.65 \text{ eV}; T \leq 400 \text{ K}.$$

The numerical model gives values of the effective migration energy that are functions of material and irradiation parameters as well as time. It is found that, at temperatures between 400 K and 600 K in nickel irradiated in typical reactor conditions, the mobility of helium is enhanced over the analytically predicted results by migration in divacancy − single helium complexes. Also, above ~ 800 K, helium mobility is less than the analytical value due to increased trapping at irradiation produced vacancies. The influence of such irradiation produced vacancies is totally negligible by ~ 1100 K.

7. Nomenclature for the rate-equations

Symbol	Description	Unit
G	Frenkel pair generation rate	(dpa/s)
G_{He}	Helium atom generation rate	(at/at/s)
G_T	Thermal vacancy generation rate	(dpa/s)
T	Temperature	(K)
P_g	Gas pressure inside a cavity	(eV/cm^3)
γ	Surface tension	(eV/cm^2)
Ω	Atomic volume	cm^3
k	Boltzmann's constant	eV K^{-1}
t	time	(s)
ε	Fraction of vacancies produced directly as divacancies by irradiation	

Symbol	Description	Unit
g	Re-solution parameter	(~ 10)
ρ_d	Line dislocation density	(cm/cm^3)
r_c	Critical growth radius	(cm)
R_{tr}	Trapping radius	(cm)
λ_α	Jump distance for defect α	(cm)
Γ_α	Jump frequency of specie α	(s^{-1})
ν_α	Vibration frequency of specie α	(s^{-1})
S_I	Self-interstitial sink strength	(cm^{-3})
S_v	Vacancy sink strength	(cm^{-3})
s_v^F	Entropy of vacancy formation	
ΔF	Free energy change due to an emission process	(eV)
D_α	Diffusion coefficient of defect α	(cm^2/s)
D_α^0	Diffusion coefficient pre-exponential for defect α	(cm^2/s)
Z_α^d	Line dislocation bias factor for defect α	
Z_α^c	Cavity bias factor for defect α	
M	Maximum number of vacancies in the ij-complex	
N	Maximum number of helium in the ij-complex	
C_v^e	Thermal equilibrium vacancy concentration	
C_I	Self-interstitial concentration	
C_{ij}	Concentration of complex containing i-vacancies and j-helium atoms	
E_{ij}^v	Emission rate constant of a vacancy from an ij-complex	(s^{-1})
B_{ij}^{He}	Emssion rate constant of a helium atom from an ij-complex	(s^{-1})
$\varepsilon^{He}(r_c)$	Helium emission rate from a cavity with radius r_c	(s^{-1})
E_α^M	Migration energy of defect α	(eV)
E_α^B	Binding energy of defect α	(eV)
E_α^F	Formation energy of defect α	(eV)
E_{He}^D	Helium detrapping energy from a substitutional site	(eV)
$R_{ij,mn}$	Reaction rate between an ij-complex and an mn-complex	(s^{-1})
$R_{I,mn}$	Reaction rate between a self-interstitial and mn-complex	(s^{-1})
R_{ij,r_c}	Reaction rate between an ij-complex and a cavity with radius r_c	(s^{-1})
$N(r_c)$	Cavity number density per unit size	(cm^{-4})
i	Number of vacancies in a cavity	
j	Number of helium atoms in a cavity	
K_{ij}^α	Combinatorial number for defect α impinging on an ij complex	

References

[1] K. Farrell, Rad. Eff. 53 (1980) 175.

[2] D.N. Braski, H. Shroeder and H. Ullmaier, J. Nucl. Mater. 83 (1979) 265.

[3] E.E. Bloom, J. Nucl. Mater. 85–86 (1979) 1025.

[4] W.D. Wilson, M.I. Baskes and C.L. Bisson, Phys. Rev. B13 (1976) 2470.

[5] M.I. Baskes, C.L. Bisson and W.D. Wilson, Sandia Lab. Report SAND-78-8836 (June 1979).

[6] C.F. Melius, W.D. Wilson and C.L. Bisson, Proc. Harwell Consultants Symposium on Inert Gases, Vol. 1 (1980) 14.

[7] V. Philipps, K. Sonnenberg and J.M. Williams, J. Nucl. Mater., to be published.

[8] V. Philipps and K. Sonnenberg, J. Nucl. Mater., to be published.

[9] D.B. Poker and J.M. Williams, Appl. Phys. Lett. 40 (1982) 851.

[10] D.J. Reed, Rad. Eff. 31 (1977) 129.

[11] L.K. Mansur, W.A. Coghlan and A.D. Brailsford, J. Nucl. Mater. 85–86 (1979) 591.

[12] S. Chandrasekhar, Rev. Mod. Phys. 15 (1943) 1.

[13] B.T.M. Loh, Acta Met. 20 (1972) 1305.

[14] K.C. Russell and D.H. Hall, Nucl. Metall. 18 (1973) 545.

[15] H. Wiedersich, J.J. Burton and J.L. Katz, J. Nucl. Mater. 51 (1974) 287.

[16] H. Wiedersich and B.O. Hall, J. Nucl. Mater. 66 (1977) 187.

[17] B.L. Eyre and R. Bullough, J. Nucl. Mater. 26 (1968) 249; also see D. Olander, NTIS publication (1976) Chapter 13.

[18] B.O. Hall, ASTM publication, Effects of Radiation on Materials: Tenth Conf. ASTM STP 725, eds., David Kramer, H.R. Brager and J.S. Perrin (American Society for Testing and Materials, 1981) p. 512.

[19] A.C. Hindmarch, Lawrence Livermore Lab. Report, UCID-3001, Rev. 3 (1974).

[20] N.M. Ghoniem and D.D. Cho, Phys. Stat. Sol. 54 (1979) 171.

[21] W.G. Wolfer and M. Ashkin, J. Appl. Phys. 46 (1975) 547.

[22] E.V. Kornelsen and A.A. Van Gorkum, J. Nucl. Mater. 92 (1980) 79.

[23] S. Sharafat and N.M. Ghoniem, to be published.

[24] N.M. Ghoniem and H. Gurol, Rad. Eff. 55 (1981) 209.

[25] W.D. Wilson and R.A. Johnson, Interaction Potentials and the Simulation of Lattice Defects, eds., C. Gehlen, R.J. Beeler and R.I. Jaffee (Plenum, New York, 1972) p. 375.

[26] N.M. Ghoniem and G.L. Kulcinski, Rad. Eff. 39 (1978) 47.

[27] A.C. Damask and G.J. Dienes, Phys. Rev. 120 (1960) 99.

[28] L.K. Mansur, Acta Met. 29 (1981) 375.